

Article

Physiological and Endophytic Fungi Changes in Grafting Seedlings of Qi-Nan Clones (*Aquilaria sinensis*)

Xiaoying Fang^{1,2}, Xiaofei Li¹, Qilei Zhang¹, Houzhen Hu¹, Zhou Hong¹ , Xiaojin Liu¹, Zhiyi Cui¹ and Daping Xu^{1,*}

¹ Research Institute of Tropical Forestry, Chinese Academy of Forestry, Guangzhou 510520, China; fangxiaoying@njfu.edu.cn (X.F.); lixiaofei@caf.ac.cn (X.L.); dalei45666@163.com (Q.Z.); hhz494@njfu.edu.cn (H.H.); hzhou1981@sina.com (Z.H.); czy@caf.ac.cn (Z.C.)

² College of Landscape Architecture, Nanjing Forestry University, Nanjing 210037, China

* Correspondence: gzfsrd@163.com

Abstract: In recent years, some new Qi-Nan clones of *Aquilaria sinensis*, which have the characteristics of easily induced and high-quality agarwood, have been selected and propagated by grafting seedlings. To date, research on the grafting of Qi-Nan seedlings is limited. In this study, the effects of grafting on physiological characteristics and endophytic fungi of seedlings within a short period after grafting were studied by means of histochemical observations, physiological index determinations and Illumina sequencing. The results showed that the grafting healing time of ordinary *A. sinensis* was at least 10 days shorter than that of Qi-Nan, according to the degree of lignification of callus, and the tissue basis for the healing was the interxylary phloem. The MDA content of Qi-Nan peaked earlier than that of ordinary *A. sinensis*. The contents of JA and ABA peaked earlier in ordinary *A. sinensis*, and the SA content was significantly higher than that of Qi-Nan at 20–40 days; on average, it was 17.33% higher than that of Qi-Nan. A total of 5 phyla, 28 classes, 84 orders, 197 families, 489 genera and 842 species of endophytic fungi were identified before and after grafting. After grafting, the abundance and diversity of endophytic fungi in ordinary *A. sinensis* and Qi-Nan decreased, and the endophytic fungi were significantly different before and after grafting. In ordinary *A. sinensis*, before grafting, *Dothideomycetes* was the dominant class, and after grafting, *Sordariomycetes* was the dominant class. The dominant class of Qi-Nan before and after grafting was *Dothideomycetes*. The dominant genus of ordinary *A. sinensis* before grafting was *Deviessia*, and after grafting, it was *Fusarium*; that of Qi-Nan before grafting was *Hyweljonesia* and after grafting was *Arthopyrenia*. Functional genes of the endophytic fungi were mostly related to carbohydrate metabolism and energy metabolism, which may be the reason why endophytic fungi promote agarwood formation in *Aquilaria* trees. The findings suggest that the healing of the grafting interface in *A. sinensis* seedlings was the result of multiple factors, and endophytic fungi of Qi-Nan scion changed after grafting.



Citation: Fang, X.; Li, X.; Zhang, Q.; Hu, H.; Hong, Z.; Liu, X.; Cui, Z.; Xu, D. Physiological and Endophytic Fungi Changes in Grafting Seedlings of Qi-Nan Clones (*Aquilaria sinensis*). *Forests* **2024**, *15*, 106. <https://doi.org/10.3390/f15010106>

Academic Editor: Otmar Urban

Received: 14 November 2023

Revised: 2 January 2024

Accepted: 3 January 2024

Published: 5 January 2024



Copyright: © 2024 by the authors. Licensee MDPI, Basel, Switzerland. This article is an open access article distributed under the terms and conditions of the Creative Commons Attribution (CC BY) license (<https://creativecommons.org/licenses/by/4.0/>).

Keywords: Qi-Nan seedlings; grafting healing; physiologic changes; Illumina sequencing

1. Introduction

Agarwood is a dark resin produced in the trunks and branches of *Aquilaria*, *Gonystylus*, and *Gyrinops* species (Thymelaeaceae). In the wild, *Aquilaria* trees will produce agarwood only when they are subjected to environmental stress, such as wounds caused by various factors, and disease and pest infections. Otherwise, healthy *Aquilaria* trees will not produce agarwood [1,2]. It has been used as incense and traditional medicines due to its unique fragrance and medicinal value [3]. Due to long-term human logging, wild *Aquilaria* species have been destructively exploited [4]. Consequently, all *Aquilaria* spp. and *Gyrinops* spp. that can produce agarwood are endangered and are listed in Appendix II of the Convention on International Trade in Endangered Species of Wild Fauna and Flora (CITES, <http://checklist.cites.org> (accessed on 12 July 2023)), including *Aquilaria sinensis* [5].

In recent years, a type of special germplasm of *Aquilaria sinensis* (Lour.) Spreng, has been selected from the wild population and used as a scion for grafting cultivation. These excellent clones, namely “Qi-Nan”, have the characteristics of more easily induced agarwood and high-quality agarwood [6–9]. For ordinary *A. sinensis*, it is almost impossible to obtain agarwood with more than 10% of the alcohol soluble extractive content only with the drilling method over one year, but this special agarwood germplasm of *A. sinensis* can have more than 40% of the alcohol soluble extractive content with the same inducing method [6].

The formation of Qi-Nan agarwood and the differences in composition between Qi-Nan agarwood and ordinary agarwood have attracted much attention [6,10–13]. Unfortunately, there are few reports of Qi-Nan grafted seedlings. Grafting is a common propagation technology. Grafting is usually used to improve the yield, quality and resistance to abiotic and biotic stresses of plants [14]. The two indispensable parts of grafting are scion and rootstock. The compatible and highly complex interaction between them determine the success of grafting, which involves the synergistic effect of hormones, metabolism, epigenetic pathways and other factors [15–17]. This intricate network of molecular mechanisms operates at the graft junction and is associated with the development and physiology of the scion [14]. Some molecular signals are bidirectionally transferred from the rootstock to the scion. Studies on the interactions between scion and rootstock have shown that there are epigenetic components in grafting reactions [18]. Epigenetic changes such as DNA methylation, histone modification, and small RNA molecules regulate the chromatin structure, leading to changes in gene expression and affecting cell function. Conversely, mobile small RNA (siRNA) migrates from rootstock to scion through graft binding, mediating the modification of DNA methylation patterns of receptor partners, leading to changes in chromatin structure and transcriptional reprogramming, thereby affecting scion traits [19]. Moreover, there is increasing evidence that signaling molecules such as hormones, nutrients, proteins and nucleic acids are transported over short or long distances through the junctions of cells near the grafting interface, or over long distances in distant receptor tissues, which is important for the success of grafts and the development and performance of scions [17,20–22]. Will the physiological characteristics of the scion change due to the influence of the rootstock after grafting?

Endophytic microbes are known to live asymptotically inside their host throughout different stages of their life cycle and play crucial roles in the growth, development, fitness, and diversification of plants. The presence of fungal endophytes increased the plant’s total biomass, chlorophyll content, and stomatal conductance. In addition, plant shoot biomass, plant height, superoxide dismutase (SOD), and phenolics were significantly increased by endophyte colonization under stressed conditions. Malondialdehyde (MDA) and hydrogen peroxide (H_2O_2) were reduced in endophytic plants under stress compared with their non-endophytic counterparts. These microbes help the host combat a diverse array of biotic and abiotic stressful conditions [23–25]. A study concluded that agarwood is the product of persistent interactions between endogenous fungi and the plant, which are triggered at the early stage of growth, and resin production is probably visible at the onset of maturity [26]. Among the endophytic fungi of the agarwood-normal transition layer, the induction ability of *Phaeoacremonium rubrigenum* to *A. sinensis* seedlings was significantly improved, especially sesquiterpenes [27].

With the lack of information about fungal diversity in *A. sinensis* seedlings and their role in fragrant resin formation, we performed Illumina sequencing to analyze endophytic fungi and observed changes in the physiological indicators of ordinary *A. sinensis* and Qi-Nan. The objective of this study was to understand the physiological changes in seedlings grafted with Qi-Nan and whether grafting would change the abundance of endophytic fungi in Qi-Nan: that is, whether there were changes before and after grafting.

2. Materials and Methods

2.1. Plant Materials and Experimental Design

The study was conducted in December 2021 at the nursery of the Research Institute of Tropical Forestry, Chinese Academy of Forestry (longitude 113.38.47 E, latitude 23.19.07 N), Guangzhou, China. Healthy one-year-old seedlings of ordinary *A. sinensis* with a ground diameter of 0.8–1.2 cm were used as rootstocks, and one-year-old branches of Qi-Nan were used as scions (QN, ordinary *A. sinensis* × Qi-Nan). In the control group, the one-year-old branches of ordinary *A. sinensis* were taken as scions for grafting (CK, ordinary *A. sinensis* × ordinary *A. sinensis*). In each treatment, fifty plants were grafted by cleft grafting, and two treatments were repeated three times across a total of 300 plants. After the grafting was completed, the samples were taken after 0, 10, 20, 30, 40, 50, 60 days, and each treatment was replicated three times, for a total of 15 plants, and the complete grafting interface was cut by scissors. Three of them were immersed in a solution containing 3% paraformaldehyde and 2% glutaraldehyde for a duration of 12 h at a temperature of 4 °C, and sections were made to observe the healing of the graft. The remaining samples were put into liquid nitrogen to determine MDA and hormone changes. Before grafting, the scions of Qi-Nan and ordinary *A. sinensis* were taken to determine the endophytic fungi. After grafting survival, the scions of Qi-Nan and ordinary *A. sinensis* were taken to determine the endophytic fungi at an interval of six months. Each treatment was repeated three times.

2.2. Graft Healing Observation

The grafting interface was cut and promptly immersed in a fixative solution containing 3% paraformaldehyde and 2% glutaraldehyde for a duration of 12 h at a temperature of 4 °C. Subsequently, the samples were subjected to three rinses in phosphate-buffered saline (PBS). The specimens were postfixed in a 1% osmium tetroxide solution for a duration of 8 h at room temperature, washed three times, dehydrated using an ethanol gradient, and subsequently embedded in Epon 812 (SPI Supplies, West Chester, PA, USA). Polymerization was carried out at temperatures of 35 °C, 40 °C, and 60 °C for a duration of 24 h each. Subsequently, the specimens underwent slicing into 15 µm sections utilizing an ultramicrotome (Leica EM UC7, Wetzlar, Germany). After being stained with safranin and fast green, the healing condition of the graft was observed. All sections were observed using a Nikon 80i light microscope (Nikon, Tokyo, Japan) [28].

2.3. Malondialdehyde (MDA) Determination

MDA was determined using a spectrophotometer [29]. For the purpose of measurement, a fresh sample weighing 0.5 g was mixed with 2.5 mL of a 5% solution of trichloroacetic acid (TCA). The resulting mixture was then subjected to centrifugation at a speed of 15,000 rpm for a duration of 20 min at a temperature of 4 °C. Subsequently, a mixture of 2 mL of the extract and 4 mL of thiobarbituric acid (TBA) solution, which contained 20% TCA, was subjected to a temperature of 100 °C for a duration of 30 min. The resulting mixture was then rapidly cooled. The spectrophotometer was used to measure the absorbance of the samples at a wavelength of 532 nm. To account for nonspecific absorbance, the readings were corrected using the absorbance recorded at 600 nm. MDA contents were quantified by employing an extinction coefficient of 156 mM cm⁻¹.

2.4. Phytohormonal Estimation

Jasmonic acid (JA), salicylic acid (SA), and abscisic acid (ABA) were measured according to Almeida Trapp et al. [30]. Stock solutions of each original phytohormone standard were prepared at 1 mg/mL in MeOH. For deuterated compounds, stock solutions were prepared in acetonitrile at 100 µg/mL. When the standard solution was prepared, the stock solution was diluted in methanol:water (7:3), and different concentrations of each hormone were determined according to the range of the calibration curve, ABA (100 µg/mL), JA and SA (200 µg/mL). The internal standard stock solutions of ABA, JA and SA were com-

bined and diluted with methanol:water (7:3) solution to make the final concentration of SA 10 ng/mL, JA and ABA 20 ng/mL and obtain the extraction solution.

Fresh plant samples (100 mg) were ground and put into test tubes, and 1 mL of ABA, JA and SA extracts containing internal standards were added. The sample was shaken for 30 min and centrifuged at 16,000 rpm at 4 °C for 5 min, and the supernatant was vacuum dried. Then, 100 µL methanol was added, and the sample was centrifuged at 16,000 rpm at 4 °C for 10 min. The supernatant was analyzed by HPLC–MS/MS.

2.5. Endogenous Fungal Properties

2.5.1. DNA Extraction and PCR Amplification

The scion samples were immersed in 75% ethanol for 1 min, 3.25% sodium hypochlorite for 3 min, 75% ethanol for 30 s, and then rinsed with sterile distilled water for 3 times to disinfect the samples' surfaces [31]. Genomic DNA was extracted directly from endophytic fungi using a modified CTAB procedure as outlined by Duong et al. [32]. Each sample was separately ground into powder with liquid nitrogen. Then, 0.5 g powder was placed in a 2 mL centrifuge tube and ground at 45 HZ (FastPrep-24 5G, MP, Santa Ana, CA, USA) for 250 s; then, it was transferred to 5 mL pre-heated (60 °C) 2× CTAB extraction buffer, which was followed by 1 h incubation at 65 °C. A NanoDrop2000 spectrophotometer (Thermo Scientific, Wilmington, DE, USA) was used to determine DNA concentration.

Primers ITS1F (5'-CTGGTCATTTAGAGGAAGTAA-3') and ITS2R (5'-GCTGCGTTCTTCATCGATGC-3') were employed for the amplification of the fungal ITS region. PCR amplification was performed using a PCR instrument (ABI GeneAmp® 9700, Foster City, CA, USA) with TransStart Fastpfu DNA Polymerase and a 20 µL reaction system. The PCR amplification conditions were as follows: pre-denaturation at 95 °C for 5 min followed by 30 s at 95 °C and 30 s at 55 °C. The following concentrations and amounts were used: 4 µL of 5 × FastPfu buffer, 2 µL of 2.5 mM dNTPs, 0.8 µL of Forward Primer (5 µM), 0.8 µL of Reverse Primer (5 µM), 0.4 µL of FastPfu Polymerase, 10 ng of Template DNA, and 2 µL of ddH₂O. After 25 cycles at 72 °C for 45 s, the PCR product was finally extended at 72 °C. Amplicons were extracted from 2% agarose gels and purified using the AxyPrep DNA Gel Extraction Kit (Axygen Biosciences, Union City, CA, USA) according to the manufacturer's instructions [31].

2.5.2. Library Construction and Sequencing

Qubit®3.0 (Life Invitrogen, Waltham, MA, USA) was used to quantify the purified PCR products, and every 24 different barcode amplicons were mixed equally. The pooled DNA product was used to construct an Illumina Pair-End library following Illumina's genomic DNA library preparation procedure. Then, the amplicon library was subjected to paired-end sequencing (2 × 250) using an Illumina MiSeq platform (Shanghai BIOZERON Co., Ltd., Shanghai, China) following established protocols. The raw reads were submitted to the NCBI Sequence Read Archive (SRA) database and assigned the Accession Number: PRJNA1026349.

2.5.3. Processing of Sequencing Data

The raw fastq files underwent demultiplexing using in-house perl scripts. This process involved utilizing the barcode sequences information for each sample and adhering to the following criteria. (a) The 250 bp reads with an average quality score < 20 over a 10 bp sliding window were truncated at the respective site. Truncated reads shorter than 50 bp were discarded. (b) Exact barcode matching was performed, allowing 2 nucleotide mismatch in primer matching. Reads containing ambiguous characters were removed. (c) Sequences that had an overlap longer than 10 bp were assembled based on their overlap sequence. Reads that could not be assembled were discarded.

OTUs were clustered with 97% similarity cutoff using UPARSE (version 7.1 <http://drive5.com/uparse/> (accessed on 2 June 2023)) and chimeric sequences were identified and removed using UCHIME (version 4.2.40) [33]. Rarefaction analysis was performed

using Mothur v.1.21.1 to assess the diversity indices, namely the Chao, ACE, and Shannon diversity indices [34]. Beta diversity analysis was conducted using the UniFrac method to compare the outcomes of the principal component analysis (PCA) performed with the community ecology package (CommEcol v.1.7.9), R-forge [35].

2.6. Data Preprocessing and Statistical Analysis

Data entry was performed using Excel 2020, and SPSS 23.0 (IBM, Armonk, NY, USA) was used for one-way ANOVA. All statistical effects were considered significant at $p < 0.05$.

3. Results

3.1. Graft Healing Situation

The healing of rootstocks grafted with *A. sinensis* was dominated by the interxylary phloem. After 10 days of grafting, most of the rootstock and scion were still in a state of separation, but some callus had been differentiated from the interxylary phloem between the rootstock and scion (Figure 1A,B). The phloem of QN was not connected, and the phloem of CK began to connect. After 20 days of grafting, a large number of callus cells were formed and proliferated rapidly. In the first 20 days, there was no significant difference between the callus of QN and CK (Figure 1C,D). After 30 days of grafting, the callus of CK was significantly greater than that of QN, and the phloem basically completed connectivity (Figure 1E,F). After 40 days of grafting, the callus of QN increased greatly, and lignification appeared in the callus of CK (Figure 1G,H). After 50 days of grafting, the healing of the grafting interface of QN and CK was basically completed. The callus of QN began to lignify, and some callus of CK had completed lignification (Figure 1I,J).

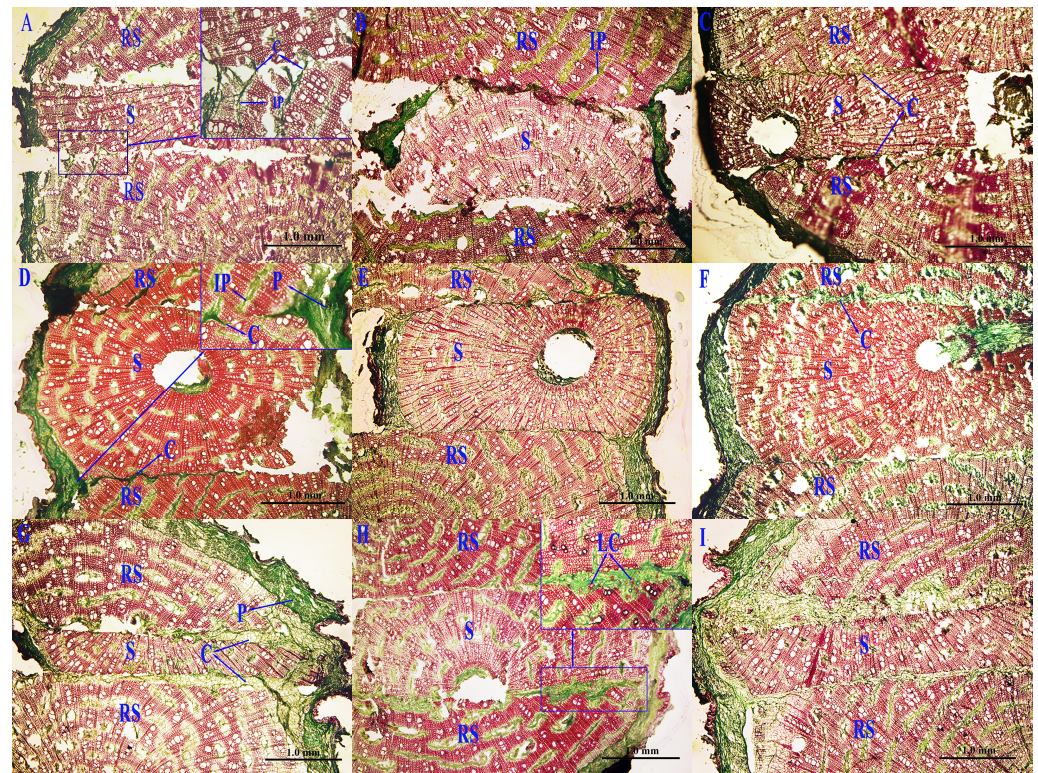


Figure 1. Cont.



Figure 1. Graft healing at different time periods. (A,C,E,G,I) show the QN graft healing condition after 10 days, 20 days, 30 days, 40 days, and 50 days, respectively; (B,D,F,H,J) show the CK graft healing condition after 10 days, 20 days, 30 days, 40 days, and 50 days, respectively; (K) Grafting began at 0 days; (L) Grafting at 50 days; RS, rootstock; S, scion; IP, interxylary phloem; C, callus; LC, lignification of callus.

3.2. Malondialdehyde (MDA) Changes in Graft Healing

The change trend of the MDA content in CK and QN was consistent at 60 days after grafting, and both showed an M shape (Figure 2). The MDA content of QN changed rapidly and peaked on the 10th and 30th days with values of 6.14 and 6.36 nmol/g, respectively, and the lowest value appeared on the 20th day. The MDA content of CK changed slowly and peaked on the 20th and 40th days with values of 6.14 and 6.44 nmol/g, respectively, and the lowest value appeared on the 30th day. The MDA content of CK and QN decreased from 40 to 60 days after grafting. The MDA of CK ranged from 5.06 to 6.16 nmol·g⁻¹, and the MDA of QN ranged from 5.30 to 6.42 nmol·g⁻¹.

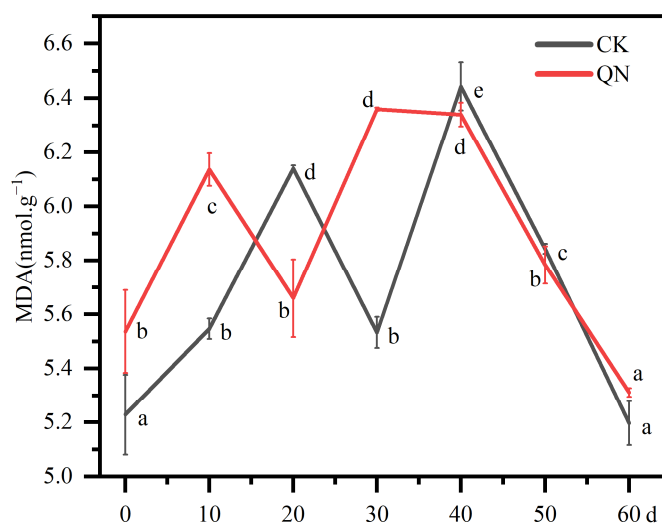


Figure 2. Malondialdehyde changes during graft healing. Different letters denote significant ($p < 0.05$) differences between CK and QN in a one-way ANOVA, and the bar represents a standard deviation ($n = 3$).

3.3. Physiological Index Changes

The change in the ethylene precursor (ACC) in QN also showed an M shape. The peak value of the ACC content in QN appeared on the 10th and 30th days with values of 204.69 and 201.31 ng/g, respectively, and the lowest value appeared on the 20th day. The content of ACC in CK continued to be higher from the 20th day to the 40th day; the peak values appeared on the 20th and 40th days with values of 200.01 and 201.83 ng/g, respectively. QN peaked earlier than CK (Figure 3A).

The content of jasmonate (JA) in QN and CK showed an M-type change trend. The change in JA in CK occurred earlier than that in QN. The first peak of QN appeared on the 20th day with a value of 1157.16 pmol/g, the first peak of CK appeared on the 10th day

with a value of 1193.47 pmol/g, the second peaks of QN and CK appeared on the 50th day with values of 1193.21 and 1188.88 pmol/g, respectively, and the lowest values of QN and CK appeared on the 30th day and the 40th day, respectively (Figure 3B).

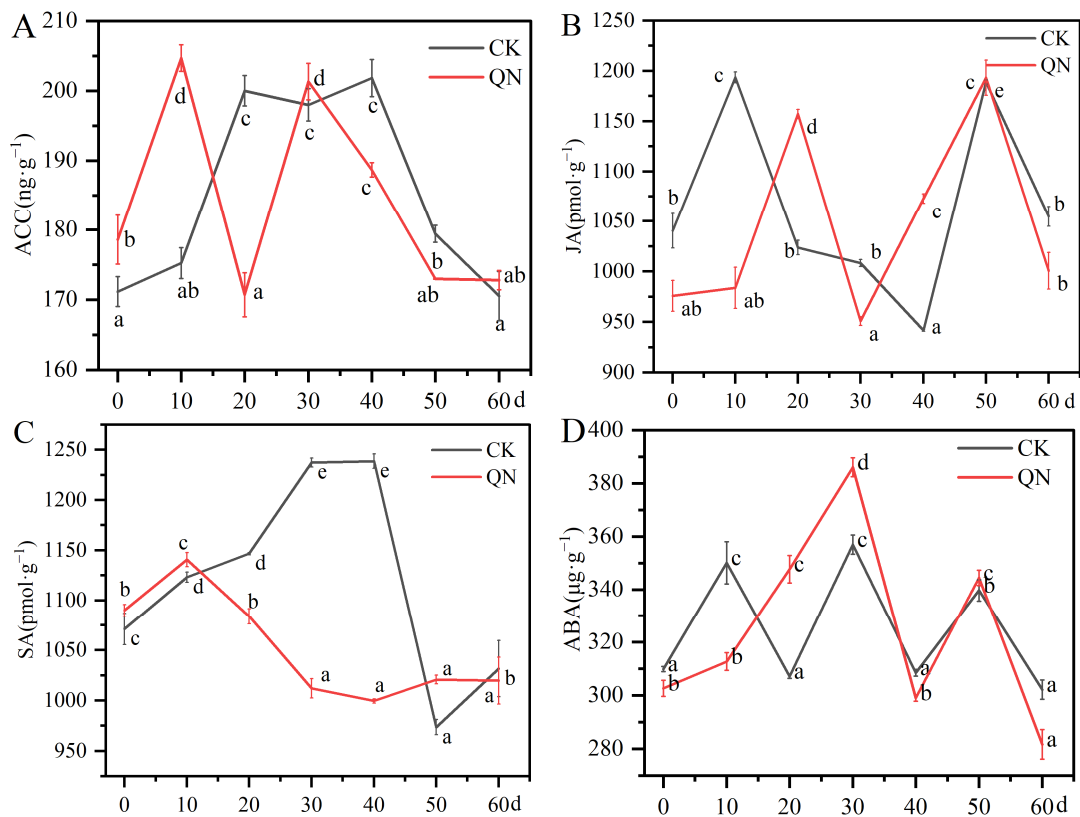


Figure 3. Physiological index changes during the graft healing process. (A) The change in ethylene precursor (ACC) content; (B) the change in jasmonate (JA) content; (C) the change in salicylic acid (SA) content; (D) the change in abscisic acid (ABA) content. Different letters denote significant ($p < 0.05$) differences between CK and QN in a one-way ANOVA, and the bar represents a standard deviation ($n = 3$).

The content of salicylic acid (SA) in QN increased to a peak in the first 10 days with a value of 1140.61 pmol/g, decreased slowly from 10 to 40 days, and increased slowly from 40 to 60 days. The content of SA in CK increased to a peak on the 30th day, remained basically unchanged from 30 to 40 days, decreased from 40 to 50 days, and increased again from 50 to 60 days. From 20 to 40 days, the content of SA in CK was much higher than that of QN with an average of 17.33% higher than that of Qi-Nan (Figure 3C).

The content of abscisic acid (ABA) in QN showed an M shape, peaking on the 30th and 50th days with values of 386.03 and 344.40 $\mu\text{g/g}$, respectively, and valleying on the 40th day. The abscisic acid content of CK peaked on the 10th day, the 30th day and the 50th day with values of 350.06, 356.93 and 339.65 $\mu\text{g/g}$, respectively, and the lowest value appeared on the 20th day and the 40th day (Figure 3D).

3.4. Endophytic Fungi Changes

3.4.1. Characterization of Sequencing Data

Endophytic fungal sequencing was performed on the control group and Qi-Nan before and after grafting. After removing the low-quality, non-fungi, potential chimeras and singletons, the remaining non-chimeric fungal internal transcribed spacer 2 (ITS2) sequences (502,234 in total) were clustered into 1638 non-singleton operational taxonomic units (OTUs) at a 97% sequence similarity level (Supplementary Materials Table S1). Among the 1638 OTUs, 1461 OTUs were identified as fungi. The fungi represented included

1184 Ascomycota, 262 Basidiomycota, 13 Mucoromycota, 1 Chytridiomycota and 1 Olpidiomycota. *Dothideomycetes*, *Sordariomycetes* and *Leotiomyces* were the major fungal groups in the endophytic fungal community of *A. sinensis*. There were significant differences in the relative abundance of endophytic fungi before and after grafting (Figure 4).

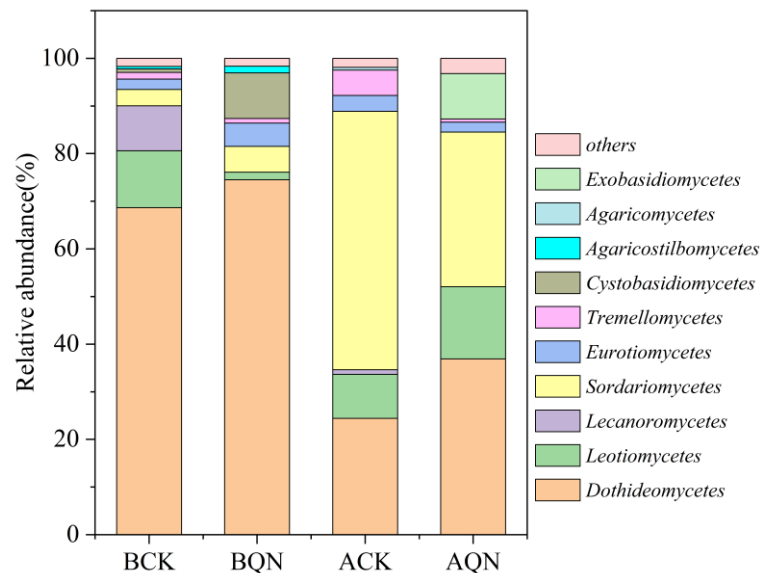


Figure 4. Relative abundance of endophytic fungi before and after grafting of *Aquilaria sinensis*. The fungal class represents <0.5% of endophytic fungi, and endophytic fungi not identified at the class level were all assigned to “Others”. BCK, before grafting of ordinary *A. sinensis*; BQN, before grafting of Qi-Nan; ACK, after grafting of ordinary *A. sinensis*; AQN, after grafting of Qi-Nan.

Alpha diversity analysis showed that there were significant differences in fungal OTU richness, Chao 1 index, ACE index and Shannon index before and after the grafting of ordinary *A. sinensis* and Qi-Nan (Figure 5A–D). The Simpson index and Pielou index of endophytic fungi before and after the grafting of ordinary *A. sinensis* were significantly different, and Qi-Nan had no significant difference in the Simpson index and Pielou index (Figure 5E,F). The results showed that the abundance and diversity of endophytic fungi in ordinary *A. sinensis* and Qi-Nan decreased after grafting (Figure 5).

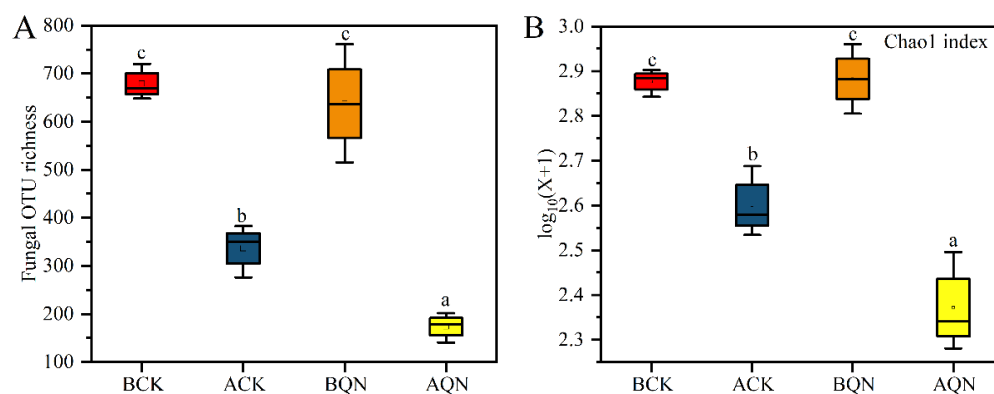


Figure 5. Cont.

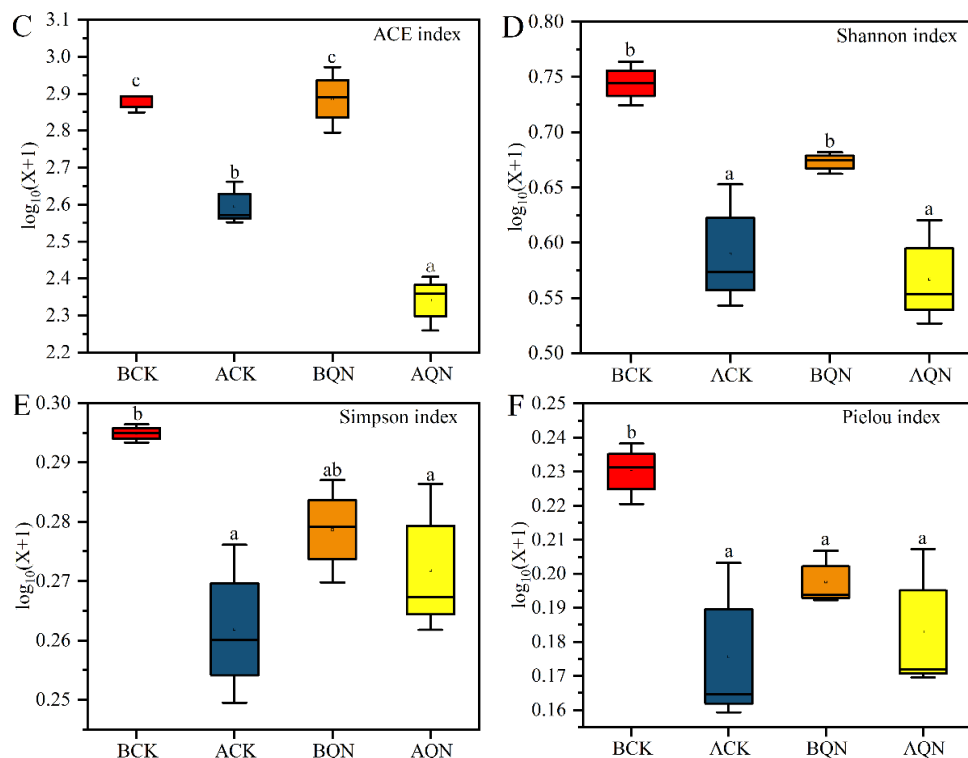


Figure 5. Alpha diversity of ordinary *A. sinensis* and Qi-Nan before and after grafting. (A) Fungal OUT richness; (B) Chao 1 index; (C) ACE index; (D) Shannon index; (E) Simpson index; (F) Pielou index. The box shows the interquartile range (IQR). The black line inside each box represents the median ($n = 3$), and the upper and lower whiskers represent the range of 1.5 times IQR beyond the upper and lower quartiles, respectively. Different letters denote significant ($p < 0.05$) differences between CK and QN in a one-way ANOVA. BCK, before grafting of ordinary *A. sinensis*; ACK, after grafting of ordinary *A. sinensis*; BQN, before grafting of Qi-Nan; AQN, after grafting of Qi-Nan.

3.4.2. Endophytic Fungi Community Structure

Analysis of Similarity (ANOSIM) showed that there were significant differences ($R = 0.96$, $p = 0.001$) in endophytic fungal communities before and after the grafting of ordinary *A. sinensis* and Qi-Nan, and there were also significant differences ($R = 0.96$, $p = 0.001$) in endophytic fungal communities between ordinary *A. sinensis* and Qi-Nan (Figure 6A). Principal component analysis (PCA) showed that the endophytic fungal community compositions of ordinary *A. sinensis* and Qi-Nan before and after grafting were significantly different (Figure 6B).

3.4.3. Community Composition of Endophytic Fungi before and after Grafting between Ordinary *A. sinensis* and Qi-Nan

A total of 5 phyla, 28 classes, 84 orders, 197 families, 489 genera and 842 species of endophytic fungi were identified before and after the grafting of ordinary *A. sinensis* and Qi-Nan. This article provides a specific analysis by class (relative abundance exceeded 0.5%). The endophytic fungi before the grafting of ordinary *A. sinensis* were *Dothideomycetes* (68.65%), *Leotiomyces* (11.97%), *Lecanoromycetes* (9.40%), *Sordariomycetes* (3.44%), *Eurotiomycetes* (2.17%), *Tremellomycetes* (1.39%), *Cystobasidiomycetes* (0.76%), and *Agaricostilbomycetes* (0.50%). After grafting, the endophytic fungi of ordinary *A. sinensis* were *Dothideomycetes* (24.41%), *Leotiomyces* (9.24%), *Lecanoromycetes* (0.97%), *Sordariomycetes* (54.25%), *Eurotiomycetes* (3.33%), *Tremellomycetes* (5.33%), and *Agaricomycetes* (0.57%). The endophytic fungi before grafting Qi-Nan were *Dothideomycetes* (74.49%), *Leotiomyces* (1.62%), *Sordariomycetes* (5.38%), *Eurotiomycetes* (4.89%), *Tremellomycetes* (0.98%), *Cystobasidiomycetes* (9.56%), and *Agaricostilbomycetes* (1.43%). After grafting, the endophytic fungi of Qi-Nan were *Dothideomycetes* (36.87%), *Leotiomyces* (15.20%), *Sordariomycetes*

(32.43%), *Eurotiomycetes* (2.10%), *Tremellomycetes* (0.65%), and *Exobasidiomycetes* (9.53%) (Figures 4 and 7).

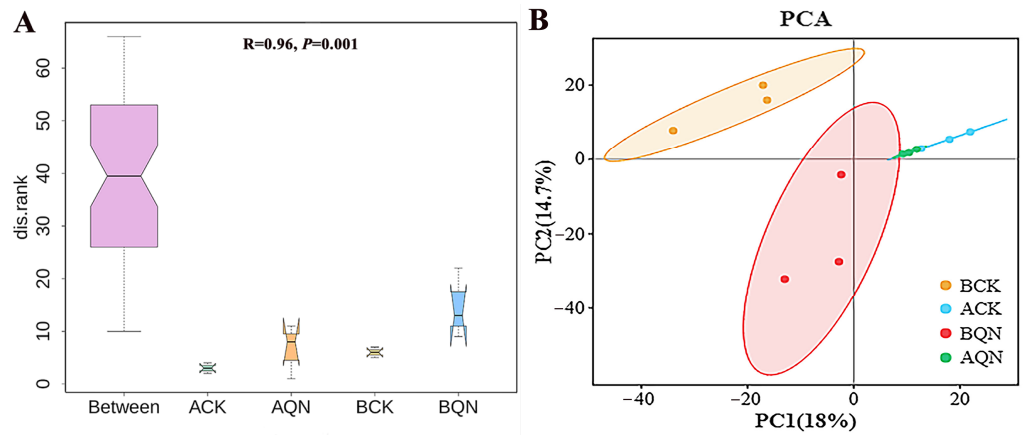


Figure 6. (A) ANOSIM and (B) PCA of endophytic fungi before and after grafting of ordinary *A. sinensis* and Qi-Nan. In (A), the box shows the interquartile range (IQR); the box thickness is the sample size; the black line inside each box represents the median, and the upper and lower whiskers represent the range of 1.5 times IQR beyond the upper and lower quartiles, respectively. Between represents the difference between groups, and others are within groups. If the slots of the boxplot do not coincide with each other, it indicates that their medians are significantly different. BCK, before grafting of or ordinary *A. sinensis*; ACK, after grafting of ordinary *A. sinensis*; BQN, before grafting of Qi-Nan; AQN, after grafting of Qi-Nan.

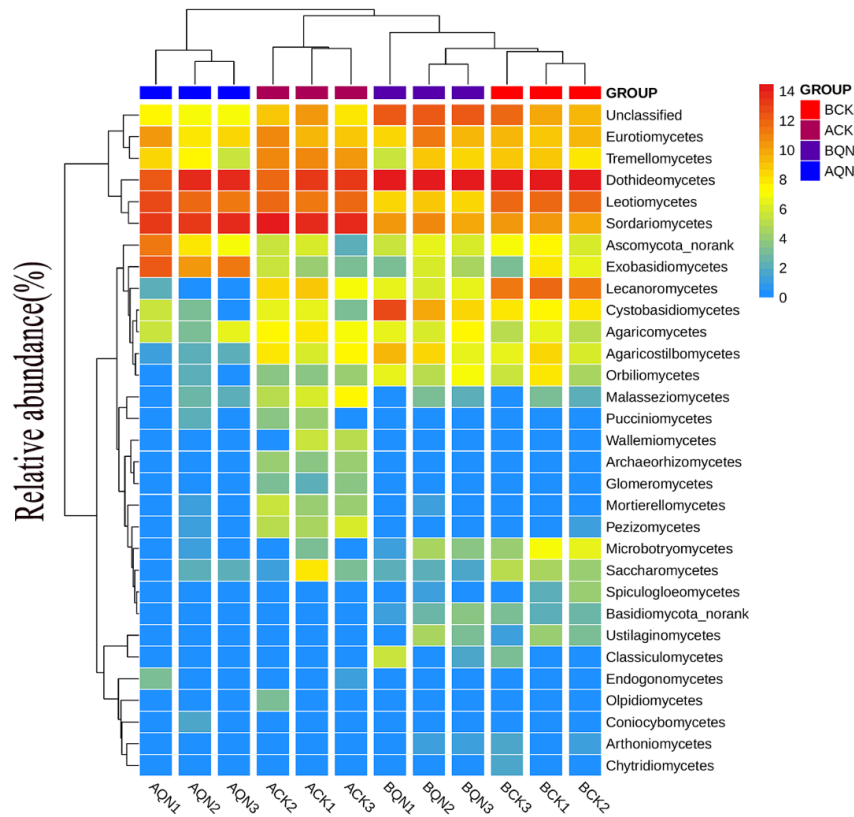


Figure 7. Heatmap depicting the distribution of relatively abundant endophytic fungi in ordinary *A. sinensis* and Qi-Nan. BCK, before grafting of or ordinary *A. sinensis*; ACK, after grafting of ordinary *A. sinensis*; BQN, before grafting of Qi-Nan; AQN, after grafting of Qi-Nan. The color of each heatmap cell indicates the relative abundance of the corresponding endophytic fungi. Cluster analysis was performed based on Bray–Curtis similarities.

At the genus level (relative abundance ranked in the top 3), the endophytic fungi before the grafting of ordinary *A. sinensis* were *Devriesia* (32.57%), *Microidium* (10.17%) and *Cryptodiscus* (9.28%). After grafting, the endophytic fungi of ordinary *A. sinensis* were *Fusarium* (35.24%), *Purpureocillium* (15.00%) and *Microidium* (9.07%). The endophytic fungi before grafting Qi-Nan were *Hyweljonesia* (14.95%), *Sporidesmajora* (11.01%) and *Occultifur* (8.50%). After grafting, the endophytic fungi of Qi-Nan were *Arthopyrenia* (26.25%), *Myrothecium* (19.38%) and *Microidium* (15.20%) (Supplementary Materials Table S2).

Before and after grafting, the endophytic fungal communities of Qi-Nan and ordinary *A. sinensis* were significantly different. In the fungal class representing $\geq 0.5\%$ of the class of endophytic fungi, there were significant differences in nine endophytic fungi, which were *Dothideomycetes*, *Leotiomyces*, *Lecanoromycetes*, *Sordariomycetes*, *Tremellomycetes*, *Cystobasidiomycetes*, *Agaricostilbomycetes*, *Agaricomycetes*, and *Exobasidiomycetes* (Figure 8).

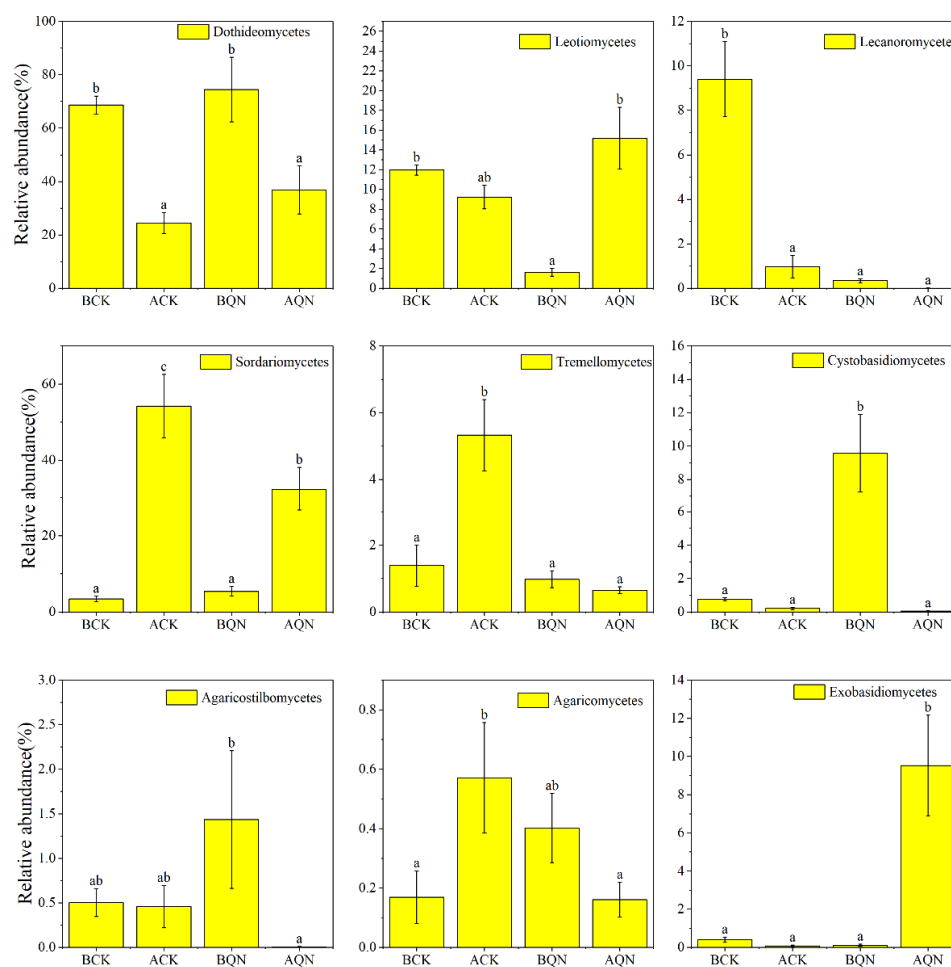


Figure 8. The difference in class level between Qi-Nan and ordinary *A. sinensis* before and after grafting. BCK, before grafting of ordinary *A. sinensis*; ACK, after grafting of ordinary *A. sinensis*; BQN, before grafting of Qi-Nan; AQN, after grafting of Qi-Nan. Different letters denote significant ($p < 0.05$) differences between CK and QN in a one-way ANOVA, and the bar represents a standard deviation ($n = 3$).

After grafting, the relative abundance of *Dothideomycetes* and *Lecanoromycetes* decreased significantly, and the relative abundance of *Sordariomycetes* increased significantly. The relative abundances of *Leotiomyces* and *Exobasidiomycetes* were not significantly different in ordinary *A. sinensis* but were significantly increased in Qi-Nan. The relative abundances of *Agaricostilbomycetes* and *Cystobasidiomycetes* were not significantly different in ordinary *A. sinensis* but decreased significantly in Qi-Nan. The relative abundance of *Tremellomycetes* increased significantly in ordinary *A. sinensis* but did not change signifi-

cantly in Qi-Nan. The relative abundance of *Agaricomycetes* was significantly increased in ordinary *A. sinensis* and significantly decreased in Qi-Nan (Figure 8).

3.4.4. Co-Occurrence Network of the Endophytic Fungal Communities

A co-occurrence network was established with OTUs of the order of ordinary *A. sinensis* and Qi-Nan endophytic fungi. The four networks consist of 120, 152, 138 and 130 edges connecting 56, 65, 52 and 35 nodes, respectively (Figure 9, Table 1). The number of nodes decreased after grafting, and the positive correlation relationship of endophytic fungi dominated. In addition, after grafting, the modularity and average path length increased, and the graph density and average degree decreased. Before grafting, the highly connected nodes of endophytic fungi were *Capnodiales* (*Dothideomycetes*), *Ostropales* (*Lecanoromycetes*), *Pleosporales* (*Dothideomycetes*), etc., in BCK and *Umbilicariales* (*Lecanoromycetes*), *Togniniales* (*Sordariomycetes*), *Trypetheliales* (*Dothideomycetes*), etc., in BQN. After grafting, the highly connected nodes of endophytic fungi were *Trichosphaeriales* (*Sordariomycetes*), *Dothideales* (*Dothideomycetes*), *Cantharellales* (*Agaricomycetes*), etc., in ACK and *Glomerellales* (*Sordariomycetes*), *Acrospemales* (*Dothideomycetes*), *Venturiales* (*Dothideomycetes*), etc., in AQN.

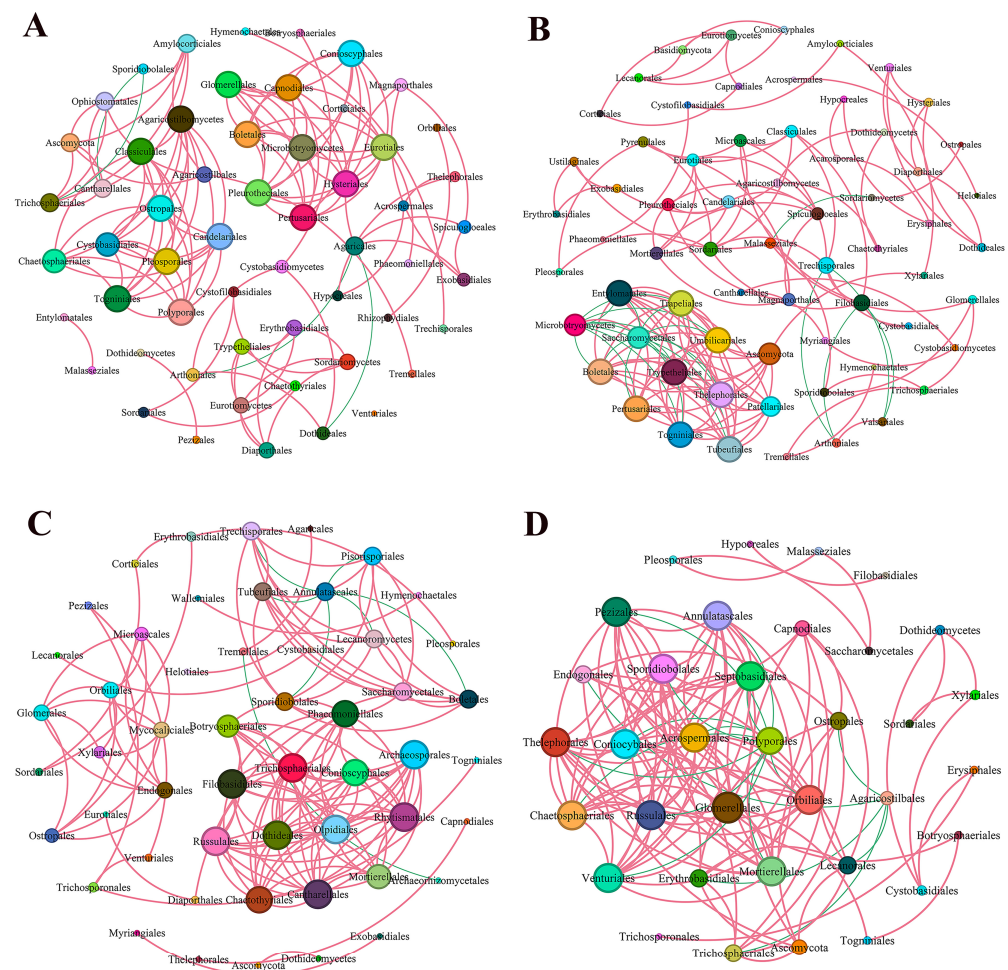


Figure 9. The co-occurrence network of the endophytic fungal communities at the order level. The networks were established by calculating correlations among OTUs. The sizes of the nodes were according to the degree of connection. The nodes of the network were colored according to different taxa. The red and green edges depicted the positive and negative correlations between endophytic fungi, respectively, as determined by Pearson correlation analysis ($p < 0.05$). The thickness of the edges is primarily determined by the correlation coefficient. (A) BCK, before grafting of ordinary *A. sinensis*; (B) BQN, before grafting of Qi-Nan; (C) ACK, after grafting of ordinary *A. sinensis*; (D) AQN, after grafting of Qi-Nan.

Table 1. Endophytic fungal community co-occurrence network of Qi-Nan and ordinary *A. sinensis* before and after grafting.

Topological Properties	BCK	BQN	ACK	AQN
Nodes	56	65	52	35
Edges	120	152	138	130
Positive (red)	96.67%	84.87%	94.93%	86.92%
Negative (green)	3.33%	15.13%	5.07%	13.08%
Average clustering coefficient	0.91	0.774	0.853	0.899
Modularity	0.809	0.947	0.648	0.529
Average path length	1.295	2.276	1.293	1.263
Network diameter	4	8	5	4
Graph density	0.078	0.073	0.104	0.218
Average degree	4.286	4.677	5.308	7.429

Note: BCK, before grafting of ordinary *A. sinensis*; ACK, after grafting of ordinary *A. sinensis*; BQN, before grafting of Qi-Nan; AQN, after grafting of Qi-Nan.

3.5. Functional Prediction of Endophytic Fungi from Ordinary *A. sinensis* and Qi-Nan

PICRUSt (Phylogenetic Investigation of Communities by Reconstruction of Unobserved States) function prediction found that the functions of endophytic fungi in ordinary *A. sinensis* and Qi-Nan were mainly divided into six aspects at level 1: Cellular processes, Environmental information processing, Genetic information processing, Human diseases, Metabolism, and Organismal systems (Figure 10). Metabolism functional genes were the most abundant, with a relative abundance of 65.31%, followed by genetic information processing, with a relative abundance of 17.47% (Supplementary Materials Table S3).

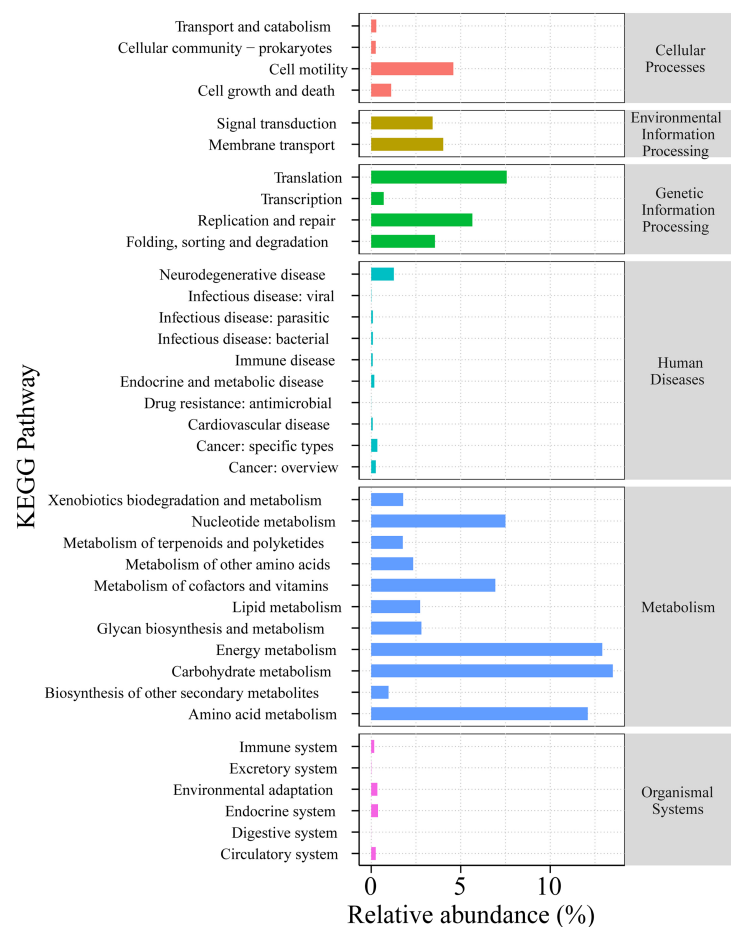


Figure 10. The PICRUSt function predicted the relative abundance of functional genes at different KEGG levels (level 1 and level 2). Columns represent the relative abundance of functional genes ($n = 3$).

PICRUSt function prediction found that the functions of endophytic fungi in ordinary *A. sinensis* and Qi-Nan were mainly divided into 37 aspects at level 2. Amino acid metabolism (12.10%), carbohydrate metabolism (13.49%) and energy metabolism (12.91%) were the three most abundant functional genes, and the differences were significant (Figure 11).

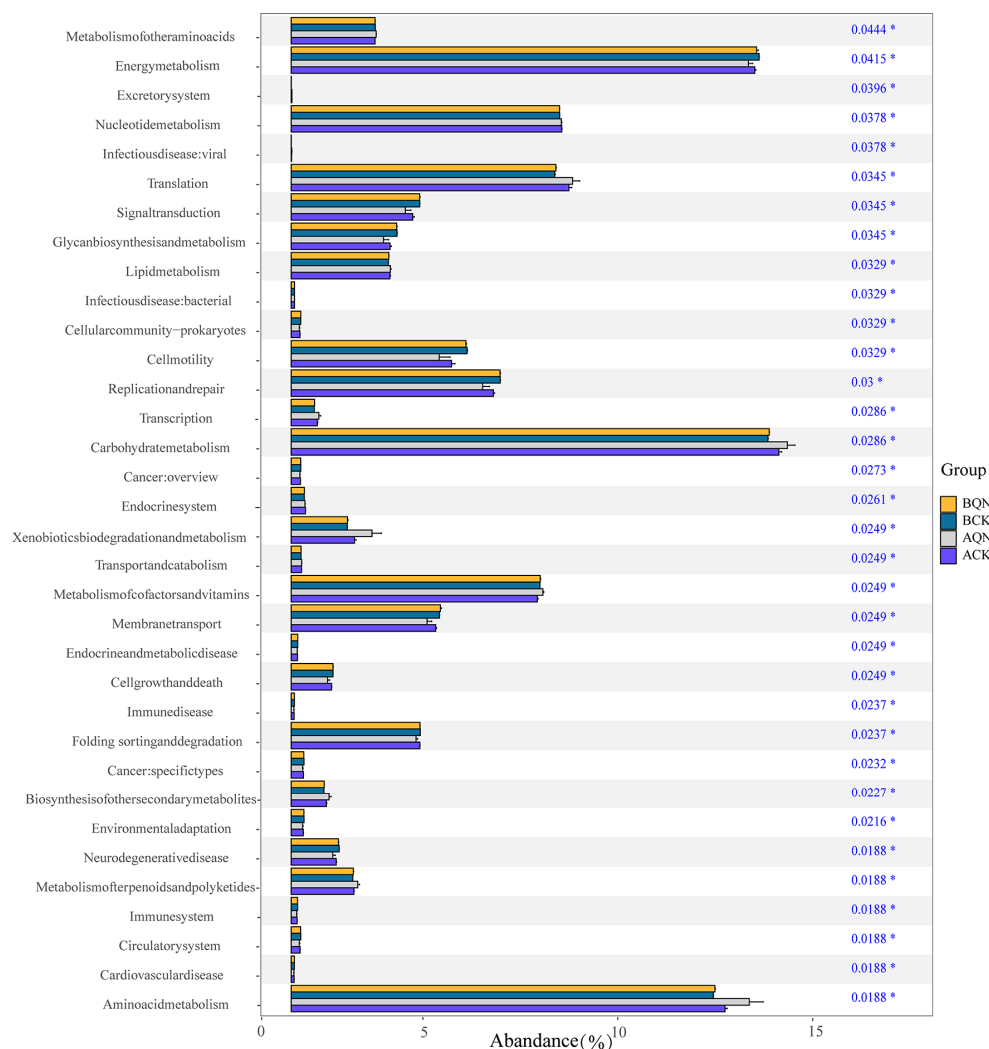


Figure 11. The functional prediction difference of endophytic fungi before and after grafting between ordinary *A. sinensis* and Qi-Nan. * represents significant difference ($p < 0.05$). BQN, before grafting of Qi-Nan; BCK, before grafting of ordinary *A. sinensis*; AQN, after grafting of Qi-Nan; ACK, after grafting of ordinary *A. sinensis*.

4. Discussion

4.1. Grafting Interface Healing

Grafting interface healing is significantly influenced by the condition of both the scion and rootstock as well as their compatibility prior to grafting. Additionally, enhanced compatibility between scion and rootstock during the grafting process results in the generation of superior grafted seedlings characterized by improved vascular connections. This compatibility also aids producers in accurately assessing the quality and timing of their production [36]. Studies have shown that both Qi-Nan and ordinary *A. sinensis* are *Aquilaria sinensis* [7], so Qi-Nan is easy to heal when ordinary *A. sinensis* is used as a grafting rootstock. However, its healing speed is not as fast as that of ordinary *A. sinensis* × ordinary *A. sinensis*.

In addition, the initial tissue cohesion between the scion and rootstock is the result of the deposition and subsequent polymerization of the cell wall material in response to wounds. For a successful graft, a coincidence between the tissues near the cambium is necessary to form a continuous connection, since the meristematic tissue between the xylem and the phloem is continuously dividing and forming new cells [37]. Interxylary phloem and xylem rays are the primary tissues that comprise living parenchyma cells in the wood of Qi-Nan and ordinary *A. sinensis*. These parenchyma cells primarily store starch grains as reserve substances [28]. The study found that the callus occurred from the interxylary phloem and xylem rays during the healing of the grafting interface in the grafting seedlings, and the interxylary phloem was the main part.

4.2. Physiological Index Changes of Grafting Seedlings

After grafting, the cell membrane was oxidized, and the MDA content increased. To maintain its own dynamic balance, severe physiological reactions occur in plants. In general, ROS production and ROS scavenging are in a state of dynamic balance. When plants are subjected to external stress, disruptions in the ROS production–scavenging cycle lead to ROS-mediated oxidative stress-induced damage. A large number of ROS accumulate in cells [38], resulting in severe peroxidation of cell membrane lipids to malondialdehyde (MDA) [39]. The accumulation of MDA inhibits the activity of antioxidant enzymes; thus, the function of the protective enzyme system is lost, and damage to the membrane system is further aggravated. During grafting, the *Aquilaria* tree was subjected to external stress, and the content of ROS increased, resulting in oxidation of the cell membrane as well as an increase in MDA content, and various hormones in the seedlings also changed. Plant growth and development and responses to biotic and abiotic stresses are regulated by plant hormones such as ethylene, auxin, gibberellin, cytokinin, salicylic acid, jasmonic acid, and abscisic acid [40]. The ethylene precursor enzyme aminocyclo-propane-1-carboxylic acid (ACC) synthesizes ethylene under the action of related enzymes [41], and ethylene was significantly correlated with the content of reactive oxygen species in plants [42]. Ethylene could also significantly reduce the accumulation of malondialdehyde and hydrogen peroxide, reduce electrolyte leakage, increase proline accumulation, enhance the activity of superoxide dismutase, peroxidase and catalase, reduce cell oxidative damage, and maintain membrane integrity and stability [43]. The ACC content of Qi-Nan seedlings increased after grafting, which increased the synthesis of ethylene extracted from plants, thus inhibiting the accumulation of MDA and hydrogen peroxide and enhancing the activity of antioxidant enzymes. The oxidative damage of the cells was reduced, and the integrity and stability of the cell membrane were maintained. It can effectively promote the healing of grafting and improve the survival rate of grafted seedlings. ABA is a key hormone in the abiotic stress response and can induce stomatal closure and reduce transpiration [44,45]. The change in ABA effectively regulated the transpiration of the Qi-Nan seedlings after grafting and avoided excessive transpiration after grafting, which led to the death of the grafted seedlings. SA plays an important role in plant resistance to biotrophic pathogens but also plays an important role in responding to abiotic stress and stimulating reactive oxygen species (ROS) signaling [46–50]. JA has been shown to effectively improve plant stress resistance under abiotic stresses [51]. It has been reported that exogenous methyl jasmonate can enhance the antioxidant enzyme activity of plants when plants are attacked [52]. The contents of SA and JA increased, and the antioxidant enzyme activity increased while transmitting the stress signal of plants to reduce the cell damage caused by stress. The physiological indices of *A. sinensis* in the study are in the process of dynamic change, which may be the result of the interaction of various hormones to maintain the dynamic balance to promote the better survival of grafted seedlings.

4.3. Endophytic Fungi of Grafting Seedlings

A large number of studies have shown that microorganisms can effectively promote the agarwood formation of *Aquilaria* trees. Among these microorganisms, endophytic fungi

have been identified as playing a crucial role in this process [2,27,53–59]. When the *Aquilaria* trees suffer from external damage, the population of endophytic fungi starts to proliferate. At the same time, the *Aquilaria* trees exhibit a response to the pathogen by initiating the synthesis of defensive metabolites that regulate the immune response. Additionally, they produce oily resins to impede or postpone the proliferation of fungi [55,60]. These oily resins are called agarwood. Endophytic fungi have a direct influence on the yield and quality of agarwood of *Aquilaria* trees.

Studies have shown that the dominant fungi isolated from *Aquilaria* plants are *Dothideomycetes* and *Sordariomycetes* [61,62]. We found that *Dothideomycetes*, *Sordariomycetes* and *Leotiomycetes* were the major endophytic fungal communities of ordinary *A. sinensis* and Qi-Nan, which was consistent with previous studies. To date, 67 endophytic genera have been isolated from *Aquilaria* and *Gyrinops*, of which 82.8% belonged to *Ascomycota* [57]. This is consistent with the results of this study, which proves that most of the fungi associated with agarwood formation in juvenile phase have existed. In addition, the dominant genera in this study are different from the genera reported except for *Fusarium*. Almost all previous studies were based on a culture-dependent approach; that is, fungi were isolated and then studied for traits and activities. However, microbes that are easy to culture in the laboratory are often not ecologically dominant or active species [63]. Another possible reason is that most of the studies are about the changes of endophytic fungi during agarwood formation, which may be different from the dominant genera of endophytic fungi of seedling.

We found that the species richness and diversity of endophytic fungi in ordinary *A. sinensis* and Qi-Nan decreased after grafting. The occurrence of physical damage following grafting induces an immune response in seedlings, leading to the production of defensive metabolites. These metabolites serve to mitigate additional damage and subsequent microbial infections. Studies have shown that these defensive metabolites have strong antibacterial properties [64–66], including functions as terpenoids, chromones and flavonoids. The main phytochemicals of agarwood include terpenoids and are dominated by sesquiterpenes. Terpenoids have been used in traditional Chinese medicine and have been shown to possess various pharmacological properties, including bacteriostatic, antibacterial, and many others [67]. Agarwood is created when *Aquilaria* trees are wounded, producing resin as a defense mechanism [68]. Therefore, in this study, grafting may activate the plant defense response and produce terpenoids. These compounds have antibacterial effects and decrease the species richness and diversity of endophytic fungi.

We also found that the endophytic fungal community compositions of ordinary *A. sinensis* and Qi-Nan before and after grafting were significantly different. External microorganisms can enter the plant by breaking down the epidermal cell wall or through wounds (including root abrasion by soil, pest damage, and wounds caused by harvesting perennials, such as *Aquilaria* spp.) [69]. After grafting, external microorganisms successfully colonized the plants after infesting them through the grafting opening, causing changes in the structure of the original endophyte community and physicochemical properties and disrupting the homeostasis of the internal environment. This may be because these exogenous fungi have a stronger ability to compete for the environment and eventually form a new homeostasis with the original endophytic fungi.

PICRUSt function prediction found that carbohydrate metabolism and energy metabolism functional genes were abundant in endophytic fungi in ordinary *A. sinensis* and Qi-Nan. Genes relevant to metabolism can influence plant growth, and beneficial microbes can synthesize and secrete secondary bioactive metabolites that maintain host plant health [70]; the endophytic fungi of Qi-Nan and ordinary *A. sinensis* perform such functions. In addition, studies have demonstrated that the process of agarwood formation involves carbohydrate metabolism in order to produce secondary metabolites. When the tree is exposed to external stress, the utilization of non-structural carbohydrates leads to the formation of agarwood [12,55]. The carbohydrate metabolism function of endophytic fungi has the potential to expedite this process and promote the formation of agarwood.

5. Conclusions

The tissue basis of grafting healing was the interxylary phloem. The grafting interface of ordinary *A. sinensis* was easier to heal than that of Qi-Nan. The response of Qi-Nan to external stress was stronger, which was the main factor for the slow healing of Qi-Nan grafting. A variety of endophytic fungi related to agarwood formation was found in grafting seedlings of Qi-Nan, and the function prediction of endophytic fungi was mostly related to carbohydrate metabolism and energy metabolism. The diversity of endophytic fungi in Qi-Nan seedlings decreased within a short period after grafting, but whether it will affect the formation and quality of agarwood in adult trees remains to be further studied.

In this study, the focus was on investigating the changes in endophytic fungi of Qi-Nan seedlings within a short period after grafting. However, it is important to note that further research is needed to examine the continuous changes in endophytic fungi in adult trees of Qi-Nan. This will help determine whether the changes in endophytic fungi after grafting in juvenile plants have any influence on the formation of agarwood in adult trees.

Supplementary Materials: The following supporting information can be downloaded at <https://www.mdpi.com/article/10.3390/f15010106/s1>, Table S1: Sequencing characteristics of Qi-Nan and ordinary *Aquilaria sinensis* samples; Table S2: The relative abundance (>1%) of endophytic fungi in Qi-Nan and ordinary *Aquilaria sinensis* at the genus level; Table S3: The KEGG pathway relative abundance statistics of each sample at level 1.

Author Contributions: Conceptualization, X.F. and X.L. (Xiaofei Li); methodology, X.F. and X.L. (Xiaofei Li); software, X.L. (Xiaofei Li) and H.H.; validation, X.F. and Z.C.; formal analysis, Q.Z. and X.F.; investigation, X.F. and X.L. (Xiaofei Li); resources, Z.H.; data curation, X.F.; writing—original draft preparation, X.F.; writing—review and editing, X.L. (Xiaofei Li) and D.X.; visualization, X.L. (Xiaojin Liu); supervision, D.X.; project administration, D.X.; funding acquisition, Z.H. All authors have read and agreed to the published version of the manuscript.

Funding: This work was supported by the Fundamental Research Funds of CAF (No: CAFYBB2021 QD003-03) and Guangzhou collaborative innovation center on science-tech of ecology and landscape (202206010058).

Data Availability Statement: All data generated during this study are included in this published article, its Supplementary Materials files and publicly available repositories. In detail, Illumina paired-end sequencing data are available in NCBI Sequence Read Archive (<http://www.ncbi.nlm.nih.gov/sra/> (accessed on 8 November 2023), Bioproject PRJNA1026349).

Acknowledgments: We thank the nursery workers at the Institute of Tropical Forestry for their help in grafting.

Conflicts of Interest: The authors declare no conflicts of interest.

References

1. Azren, P.D.; Lee, S.Y.; Emang, D.; Mohamed, R. History and Perspectives of Induction Technology for Agarwood Production from Cultivated *Aquilaria* in Asia: A Review. *J. For. Res.* **2019**, *30*, 1–11. [[CrossRef](#)]
2. Chen, X.Y.; Sui, C.; Liu, Y.Y.; Yang, Y.; Liu, P.W.; Zhang, Z.; Wei, J.H. Agarwood Formation Induced by Fermentation Liquid of *Lasioidiplodia Theobromae*, the Dominating Fungus in Wounded Wood of *Aquilaria sinensis*. *Curr. Microbiol.* **2017**, *74*, 460–468. [[CrossRef](#)] [[PubMed](#)]
3. Gao, M.; Han, X.M.; Sun, Y.; Chen, H.J.; Yang, Y.; Liu, Y.; Meng, H.; Gao, Z.; Xu, Y.; Zhang, Z.; et al. Overview of Sesquiterpenes and Chromones of Agarwood Originating from Four Main Species of the Genus *Aquilaria*. *RSC Adv.* **2019**, *9*, 4113–4130. [[CrossRef](#)] [[PubMed](#)]
4. Wu, Z.Q.; Liu, W.Z.; Li, J.; Yu, L.; Lin, L. Dynamic Analysis of Gene Expression and Determination of Chemicals in Agarwood in *Aquilaria sinensis*. *J. For. Res.* **2020**, *31*, 1833–1841. [[CrossRef](#)]
5. Liu, J.; Yang, J.; Jiang, C.; Zhou, J.H.; Zhao, Y.Y.; Huang, L.Q. Volatile Organic Compound and Endogenous Phytohormone Characteristics during Callus Browning in *Aquilaria sinensis*. *Ind. Crops Prod.* **2021**, *168*, 113605. [[CrossRef](#)]
6. Yu, M.; Liu, Y.Y.; Feng, J.; Chen, D.L.; Yang, Y.; Liu, P.; Yu, Z.; Wei, J. Remarkable Phytochemical Characteristics of Chi-Nan Agarwood Induced from New-Found Chi-Nan Germplasm of *Aquilaria sinensis* Compared with Ordinary Agarwood. *Int. J. Anal. Chem.* **2021**, *2021*, 5593730. [[CrossRef](#)]

7. Hou, W.C.; Liu, P.W.; Liu, Y.Y.; Kang, Y.; Yang, Y.; Zhang, Y.; Gao, Z.; Yu, M.; Feng, J.; Lv, F.; et al. Chi-Nan Agarwood Germplasms Constitute a New Chemotype of *Aquilaria sinensis* (Lour.) Spreng. *Ind. Crops Prod.* **2022**, *187*, 115494. [[CrossRef](#)]
8. Kang, Y.; Liu, P.W.; Lv, F.F.; Zhang, Y.X.; Yang, Y.; Wei, J.H. Genetic Relationship and Source Species Identification of 58 Qi-Nan Germplasms of *Aquilaria* Species in China That Easily Form Agarwood. *PLoS ONE* **2022**, *17*, e0270167. [[CrossRef](#)]
9. Zhang, P.; Li, X.F.; Cui, Z.Y.; Xu, D.P. Morphological, Physiological, Biochemical and Molecular Analyses Reveal Wounding-Induced Agarwood Formation Mechanism in Two Types of *Aquilaria sinensis* (Lour.) Spreng. *Ind. Crops Prod.* **2022**, *178*, 114603. [[CrossRef](#)]
10. Chen, Y.; Yan, T.T.; Zhang, Y.G.; Wang, Q.; Li, G.Y. Characterization of the Incense Ingredients of Cultivated Grafting Kynam by TG-FTIR and HS-GC-MS. *Fitoterapia* **2020**, *142*, 104493. [[CrossRef](#)]
11. Li, W.; Chen, H.Q.; Wang, H.; Mei, W.L.; Dai, H.F. Natural Products in Agarwood and *Aquilaria* Plants: Chemistry, Biological Activities and Biosynthesis. *Nat. Prod. Rep.* **2021**, *38*, 528–565. [[CrossRef](#)] [[PubMed](#)]
12. Li, X.F.; Cui, Z.Y.; Liu, X.J.; Hong, Z.; Zhang, P.; Xu, D.P. Comparative Morphological, Anatomical and Physiological Analyses Explain the Difference of Wounding-Induced Agarwood Formation between Ordinary Agarwood Nongrafted Plants and Five Grafted Qi-Nan Clones (*Aquilaria sinensis*). *Forests* **2022**, *13*, 1618. [[CrossRef](#)]
13. Yang, L.; Yang, J.L.; Dong, W.H.; Wang, Y.L.; Zeng, J.; Yuan, J.Z.; Wang, H.; Mei, W.L.; Dai, H.F. The Characteristic Fragrant Sesquiterpenes and 2-(2-Phenylethyl)Chromones in Wild and Cultivated “Qi-Nan” Agarwood. *Mol. Basel Switz.* **2021**, *26*, 436. [[CrossRef](#)] [[PubMed](#)]
14. Kapazoglou, A.; Tani, E.; Avramidou, E.V.; Abraham, E.M.; Gerakari, M.; Megariti, S.; Doupis, G.; Doulis, A.G. Epigenetic Changes and Transcriptional Reprogramming Upon Woody Plant Grafting for Crop Sustainability in a Changing Environment. *Front. Plant Sci.* **2020**, *11*, 613004. [[CrossRef](#)] [[PubMed](#)]
15. Gautier, A.T.; Chambaud, C.; Brocard, L.; Ollat, N.; Gambetta, G.A.; Delrot, S.; Cookson, S.J. Merging Genotypes: Graft Union Formation and Scion-Rootstock Interactions. *J. Exp. Bot.* **2019**, *70*, 747–755. [[CrossRef](#)]
16. Melnyk, C.W.; Schuster, C.; Leyser, O.; Meyerowitz, E.M. A Developmental Framework for Graft Formation and Vascular Reconnection in Arabidopsis Thaliana. *Curr. Biol.* **2015**, *25*, 1306–1318. [[CrossRef](#)] [[PubMed](#)]
17. Sharma, A.; Zheng, B.S. Molecular Responses during Plant Grafting and Its Regulation by Auxins, Cytokinins, and Gibberellins. *Biomolecules* **2019**, *9*, 397. [[CrossRef](#)] [[PubMed](#)]
18. Kapazoglou, A.; Ganopoulos, I.; Tani, E.; Tsaftaris, A. Epigenetics, Epigenomics and Crop Improvement. In *Advances in Botanical Research*; Kuntz, M., Ed.; Transgenic Plants; Academic Press: Cambridge, MA, USA, 2018; Volume 86, pp. 287–324.
19. Wang, W.Q.; Allan, A.; Yin, X.R. Small RNAs With a Big Impact on Horticultural Traits. *Crit. Rev. Plant Sci.* **2020**, *39*, 30–43. [[CrossRef](#)]
20. Gaut, B.S.; Miller, A.J.; Seymour, D.K. Living with Two Genomes: Grafting and Its Implications for Plant Genome-to-Genome Interactions, Phenotypic Variation, and Evolution. *Annu. Rev. Genet.* **2019**, *53*, 195–215. [[CrossRef](#)]
21. Nanda, A.K.; Melnyk, C.W. The Role of Plant Hormones during Grafting. *J. Plant Res.* **2018**, *131*, 49–58. [[CrossRef](#)]
22. Thomas, H.R.; Frank, M.H. Connecting the Pieces: Uncovering the Molecular Basis for Long-Distance Communication through Plant Grafting. *New Phytol.* **2019**, *223*, 582–589. [[CrossRef](#)] [[PubMed](#)]
23. Adeleke, B.S.; Babalola, O.O.; Glick, B.R. Plant Growth-Promoting Root-Colonizing Bacterial Endophytes. *Rhizosphere* **2021**, *20*, 100433. [[CrossRef](#)]
24. Dastogeer, K.M.G. Influence of Fungal Endophytes on Plant Physiology Is More Pronounced under Stress than Well-Watered Conditions: A Meta-Analysis. *Planta* **2018**, *248*, 1403–1416. [[CrossRef](#)] [[PubMed](#)]
25. Rana, K.L.; Kour, D.; Kaur, T.; Devi, R.; Yadav, A.N.; Yadav, N.; Dhaliwal, H.S.; Saxena, A.K. Endophytic Microbes: Biodiversity, Plant Growth-Promoting Mechanisms and Potential Applications for Agricultural Sustainability. *Antonie Van Leeuwenhoek* **2020**, *113*, 1075–1107. [[CrossRef](#)] [[PubMed](#)]
26. Mochahari, D.; Kharnaigor, S.; Sen, S.; Thomas, S. Isolation of Endophytic Fungi from Juvenile *Aquilaria malaccensis* and Their Antimicrobial Properties. *J. Trop. For. Sci.* **2020**, *32*, 97–104. [[CrossRef](#)]
27. Liu, J.; Li, T.X.; Chen, T.; Gao, J.Q.; Zhang, X.; Jiang, C.; Yang, J.; Zhou, J.; Wang, T.; Chi, X.; et al. Integrating Multiple Omics Identifies Phaeoacremonium Rubrigenum Acting as *Aquilaria sinensis* Marker Fungus to Promote Agarwood Sesquiterpene Accumulation by Inducing Plant Host Phosphorylation. *Microbiol. Spectr.* **2022**, *10*, e0272221. [[CrossRef](#)] [[PubMed](#)]
28. Liu, P.W.; Zhang, X.L.; Yang, Y.; Sui, C.; Xu, Y.H.; Wei, J.H. Interxylary Phloem and Xylem Rays Are the Structural Foundation of Agarwood Resin Formation in the Stems of *Aquilaria sinensis*. *Trees* **2019**, *33*, 533–542. [[CrossRef](#)]
29. Farsaraei, S.; Mehdizadeh, L.; Moghaddam, M. Seed Priming with Putrescine Alleviated Salinity Stress During Germination and Seedling Growth of Medicinal Pumpkin. *J. Soil Sci. Plant Nutr.* **2021**, *21*, 1782–1792. [[CrossRef](#)]
30. Almeida Trapp, M.; De Souza, G.D.; Rodrigues-Filho, E.; Boland, W.; Mithöfer, A. Validated Method for Phytohormone Quantification in Plants. *Front. Plant Sci.* **2014**, *5*, 417. [[CrossRef](#)]
31. Yao, H.; Sun, X.; He, C.; Maitra, P.; Li, X.-C.; Guo, L.-D. Phyllosphere Epiphytic and Endophytic Fungal Community and Network Structures Differ in a Tropical Mangrove Ecosystem. *Microbiome* **2019**, *7*, 57. [[CrossRef](#)]
32. Duong, L.; Jeewon, R.; Lumyong, S. DGGE Coupled with Ribosomal DNA Gene Phylogenies Reveal Uncharacterized Fungal Phylotypes. *Fungal Divers.* **2006**, *23*, 121–138.

33. Amato, K.R.; Yeoman, C.J.; Kent, A.; Righini, N.; Carbonero, F.; Estrada, A.; Gaskins, H.R.; Stumpf, R.M.; Yildirim, S.; Torralba, M.; et al. Habitat Degradation Impacts Black Howler Monkey (*Alouatta pigra*) Gastrointestinal Microbiomes. *ISME J.* **2013**, *7*, 1344–1353. [[CrossRef](#)] [[PubMed](#)]
34. Schloss, P.D.; Westcott, S.L.; Ryabin, T.; Hall, J.R.; Hartmann, M.; Hollister, E.B.; Lesniewski, R.A.; Oakley, B.B.; Parks, D.H.; Robinson, C.J.; et al. Introducing Mothur: Open-Source, Platform-Independent, Community-Supported Software for Describing and Comparing Microbial Communities. *Appl. Environ. Microbiol.* **2009**, *75*, 7537–7541. [[CrossRef](#)] [[PubMed](#)]
35. Lozupone, C.; Lladser, M.E.; Knights, D.; Stombaugh, J.; Knight, R. UniFrac: An Effective Distance Metric for Microbial Community Comparison. *ISME J.* **2011**, *5*, 169–172. [[CrossRef](#)] [[PubMed](#)]
36. Bantis, F.; Koukounaras, A.; Siomos, A.S.; Dangitsis, C. Impact of Scion and Rootstock Seedling Quality Selection on the Vigor of Watermelon–Interspecific Squash Grafted Seedlings. *Agriculture* **2020**, *10*, 326. [[CrossRef](#)]
37. Baron, D.; Esteves Amaro, A.C.; Pina, A.; Ferreira, G. An Overview of Grafting Re-Establishment in Woody Fruit Species. *Sci. Hortic.* **2019**, *243*, 84–91. [[CrossRef](#)]
38. Choudhary, A.; Kumar, A.; Kaur, N. ROS and Oxidative Burst: Roots in Plant Development. *Plant Divers.* **2019**, *42*, 33–43. [[CrossRef](#)]
39. Mi, Y.F.; Ma, X.W.; Chen, S.C. Resistant Evaluation of Kiwifruit Rootstocks to Root Zone Hypoxia Stress. *Am. J. Plant Sci.* **2013**, *4*, 945–954. [[CrossRef](#)]
40. Reckova, S.; Tuma, J.; Dobrev, P.; Vankova, R. Influence of Copper on Hormone Content and Selected Morphological, Physiological and Biochemical Parameters of Hydroponically Grown *Zea mays* Plants. *Plant Growth Regul.* **2019**, *89*, 191–201. [[CrossRef](#)]
41. Husain, T.; Fatima, A.; Suhel, M.; Singh, S.; Sharma, A.; Prasad, S.M.; Singh, V.P. A Brief Appraisal of Ethylene Signaling under Abiotic Stress in Plants. *Plant Signal. Behav.* **2020**, *15*, 1782051. [[CrossRef](#)]
42. Iqbal, N.; Khan, N.A.; Ferrante, A.; Trivellini, A.; Francini, A.; Khan, M.I.R. Ethylene Role in Plant Growth, Development and Senescence: Interaction with Other Phytohormones. *Front. Plant Sci.* **2017**, *8*, 475. [[CrossRef](#)] [[PubMed](#)]
43. Yu, Y.W.; Wang, J.; Li, S.H.; Kakan, X.; Zhou, Y.; Miao, Y.; Wang, F.; Qin, H.; Huang, R. Ascorbic Acid Integrates the Antagonistic Modulation of Ethylene and Abscisic Acid in the Accumulation of Reactive Oxygen Species. *Plant Physiol.* **2019**, *179*, 1861–1875. [[CrossRef](#)] [[PubMed](#)]
44. Bucker-Neto, L.; Paiva, A.; Machado, R.; Arenhart, R.; Margis-Pinheiro, M. Interactions between Plant Hormones and Heavy Metals Responses. *Genet. Mol. Biol.* **2017**, *40*, 373–386. [[CrossRef](#)] [[PubMed](#)]
45. Sharma, S.; Kumar, V. Responses of Wild Type and Abscisic Acid Mutants of *Arabidopsis thaliana* to Cadmium. *J. Plant Physiol.* **2002**, *159*, 1323–1327. [[CrossRef](#)]
46. Grant, M.; Lamb, C. Systemic Immunity. *Curr. Opin. Plant Biol.* **2006**, *9*, 414–420. [[CrossRef](#)] [[PubMed](#)]
47. Ke, Y.G.; Liu, H.B.; Li, X.H.; Xiao, J.H.; Wang, S.P. Rice OsPAD4 Functions Differently from *Arabidopsis* AtPAD4 in Host-Pathogen Interactions. *Plant J.* **2014**, *78*, 619–631. [[CrossRef](#)] [[PubMed](#)]
48. Xu, L.; Zhao, H.Y.; Ruan, W.Y.; Deng, M.J.; Wang, F.; Peng, J.; Luo, J.; Chen, Z.; Yi, K. ABNORMAL INFLORESCENCE MERISTEM1 Functions in Salicylic Acid Biosynthesis to Maintain Proper Reactive Oxygen Species Levels for Root Meristem Activity in Rice. *Plant Cell* **2017**, *29*, 560–574. [[CrossRef](#)]
49. Yang, L.; Li, B.S.; Zheng, X.Y.; Li, J.G.; Yang, M.; Dong, X.; He, G.; An, C.; Deng, X.W. Salicylic Acid Biosynthesis is Enhanced and Contributes to Increased Biotrophic Pathogen Resistance in *Arabidopsis* hybrids. *Nat. Commun.* **2015**, *6*, 7309. [[CrossRef](#)]
50. Zhou, X.T.; Jia, L.J.; Wang, H.J.; Zhao, P.; Wang, W.Y.; Liu, N.; Song, S.-W.; Wu, Y.; Su, L.; Zhang, J.; et al. The Potato Transcription Factor StbZIP61 Regulates Dynamic Biosynthesis of Salicylic Acid in Defense against *Phytophthora infestans* Infection. *Plant J.* **2018**, *95*, 1055–1068. [[CrossRef](#)]
51. Bali, S.G.; Kaur, P.; Kohli, S.K.; Ohri, P.; Thukral, A.K.; Bhardwaj, R.; Wijaya, L.; Alyemeni, Ahmad, P. Jasmonic Acid Induced Changes in Physio-Biochemical Attributes and Ascorbate–Glutathione Pathway in *Lycopersicon esculentum* under Lead Stress at Different Growth Stages. *Sci. Total Environ.* **2018**, *645*, 1344–1360. [[CrossRef](#)]
52. Hanaka, A.; Lechowski, L.; Mroczek-Zdyrska, M.; Strubińska, J. Oxidative Enzymes Activity during Abiotic and Biotic Stresses in *Zea Mays* Leaves and Roots Exposed to Cu, Methyl Jasmonate and *Trigonotylus caelestialium*. *Physiol. Mol. Biol. Plants Int. J. Funct. Plant Biol.* **2018**, *24*, 1–5. [[CrossRef](#)] [[PubMed](#)]
53. Du, T.Y.; Dao, C.J.; Mapook, A.; Stephenson, S.L.; Elgorban, A.M.; Al-Rejaie, S.; Suwannarach, N.; Karunarathna, S.C.; Tibpromma, S. Diversity and Biosynthetic Activities of Agarwood Associated Fungi. *Diversity* **2022**, *14*, 211. [[CrossRef](#)]
54. Nagajothi, M.S.; Parthiban, K.T.; Kanna, S.U.; Karthiba, L.; Saravanakumar, D. Fungal Microbes Associated with Agarwood Formation. *Am. J. Plant Sci.* **2016**, *7*, 1445–1452. [[CrossRef](#)]
55. Cui, J.; Guo, S.; Fu, S.; Xiao, P.; Wang, M. Effects of Inoculating Fungi on Agarwood Formation in *Aquilaria sinensis*. *Chin. Sci. Bull.* **2013**, *58*, 3280–3287. [[CrossRef](#)]
56. Siburian, R.H.; Siregar, U.J.; Siregar, I.Z.; Santoso, E. Identification of Morphological Characters of *Aquilaria microcarpa* in the Interaction with *Fusarium solani*. *Int. J. Sci. Basic Appl. Res.* **2015**, *20*, 119–128.
57. Li, T.X.; Qiu, Z.D.; Yih Lee, S.; Li, X.; Gao, J.Q.; Jiang, C.; Huang, L.; Liu, J. Biodiversity and Application Prospects of Fungal Endophytes in the Agarwood-Producing Genera, *Aquilaria* and *Gyrinops* (Thymelaeaceae): A Review. *Arab. J. Chem.* **2023**, *16*, 104435. [[CrossRef](#)]
58. Sen, S.; Dehingia, M.; Talukdar, N.C.; Khan, M. Chemometric Analysis Reveals Links in the Formation of Fragrant Bio-Molecules during Agarwood (*Aquilaria malaccensis*) and Fungal Interactions. *Sci. Rep.* **2017**, *7*, 44406. [[CrossRef](#)]

59. Xu, Y.H.; Zhang, Z.; Wang, M.X.; Wei, J.H.; Chen, H.J.; Gao, Z.; Sui, C.; Luo, H.; Zhang, X.; Yang, Y.; et al. Identification of Genes Related to Agarwood Formation: Transcriptome Analysis of Healthy and Wounded Tissues of *Aquilaria sinensis*. *BMC Genomics* **2013**, *14*, 227. [[CrossRef](#)]
60. Chhipa, H.; Kaushik, N. Fungal and Bacterial Diversity Isolated from *Aquilaria malaccensis* Tree and Soil, Induces Agarospirol Formation within 3 Months after Artificial Infection. *Front. Microbiol.* **2017**, *8*, 1286. [[CrossRef](#)]
61. Premalatha, K.; Kalra, A. Molecular Phylogenetic Identification of Endophytic Fungi Isolated from Resinous and Healthy Wood of *Aquilaria malaccensis*, a Red Listed and Highly Exploited Medicinal Tree. *Fungal Ecol.* **2013**, *6*, 205–211. [[CrossRef](#)]
62. Rasool, S.; Mohamed, R. Understanding Agarwood Formation and Its Challenges. In *Agarwood: Science Behind the Fragrance*; Mohamed, R., Ed.; Springer: Berlin, Germany, 2016; pp. 39–56. [[CrossRef](#)]
63. Rastogi, G.; Sani, R.K. Molecular Techniques to Assess Microbial Community Structure, Function, and Dynamics in the Environment. In *Microbes and Microbial Technology*; Iqbal, A., Farah, A., John, P., Eds.; Springer: New York, NY, USA, 2011; pp. 29–57.
64. Dahham, S.S.; Tabana, Y.M.; Iqbal, M.A.; Ahamed, M.B.K.; Ezzat, M.O.; Majid, A.S.A.; Majid, A.M.S.A. The Anticancer, Antioxidant and Antimicrobial Properties of the Sesquiterpene β -Caryophyllene from the Essential Oil of *Aquilaria crassna*. *Molecules* **2015**, *20*, 11808–11829. [[CrossRef](#)] [[PubMed](#)]
65. Li, W.; Cai, C.H.; Dong, W.H.; Guo, Z.K.; Wang, H.; Mei, W.L.; Dai, H.F. 2-(2-Phenylethyl)Chromone Derivatives from Chinese Agarwood Induced by Artificial Holing. *Fitoterapia* **2014**, *98*, 117–123. [[CrossRef](#)] [[PubMed](#)]
66. Wang, H.N.; Dong, W.H.; Huang, S.Z.; Li, W.; Kong, F.D.; Wang, H.; Wang, J.; Mei, W.-L.; Dai, H.-F. Three New Sesquiterpenoids from Agarwood of *Aquilaria crassna*. *Fitoterapia* **2016**, *114*, 7–11. [[CrossRef](#)] [[PubMed](#)]
67. Wang, Y.C.; Hussain, M.; Jiang, Z.B.; Wang, Z.H.; Gao, J.; Ye, F.; Mao, R.; Li, H. *Aquilaria* Species (Thymelaeaceae) Distribution, Volatile and Non-Volatile Phytochemicals, Pharmacological Uses, Agarwood Grading System, and Induction Methods. *Molecules* **2021**, *26*, 7708. [[CrossRef](#)]
68. Shivanand, P.; Arbie, N.; Krishnamoorthy, S.; Ahmad, N. Agarwood—The Fragrant Molecules of a Wounded Tree. *Molecules* **2022**, *27*, 3386. [[CrossRef](#)]
69. Schulz, B.; Boyle, C. The Endophytic Continuum. *Mycol. Res.* **2005**, *109*, 661–686. [[CrossRef](#)]
70. Xia, A.N.; Liu, J.; Kang, D.C.; Zhang, H.G.; Zhang, R.H.; Liu, Y.G. Assessment of Endophytic Bacterial Diversity in Rose by High-Throughput Sequencing Analysis. *PLoS ONE* **2020**, *15*, e0230924. [[CrossRef](#)]

Disclaimer/Publisher's Note: The statements, opinions and data contained in all publications are solely those of the individual author(s) and contributor(s) and not of MDPI and/or the editor(s). MDPI and/or the editor(s) disclaim responsibility for any injury to people or property resulting from any ideas, methods, instructions or products referred to in the content.